[2] Reissner, E., "A new derivation of the equations for the deformation of elastic shells," Am. J. Math. **63**, 177–184 (1941).

[3] Sepetoski, W. K., Pearson, C. E., Dingwell, I. W., and Adkins, A. W., "A digital computer program for the general axially symmetric thin shell problem," J. Appl. Mech. **29**, 655–661 (1962).

[4] Timoshenko, S. and Woinowsky-Krieger, S., *Theory of Plates and Shells* (McGraw-Hill Book Co., Inc., New York, 1959), 2nd ed., pp. 534–535.

[5] Wittrick, W. H., "Interaction between membrane and edge stresses for thin cylinders under axially symmetrical loading," J. Roy. Aeron. Soc. **67**, 172–174 **30**, (1963).

[6] Cline, G. B., "Effect of internal pressure on the influence coefficients of spherical shells," J. Appl. Mech. **30**, 91–97 (1963).

[7] Wei, B. C. F., "Structural analysis of solid propellant rocket casings," ARS Preprint 1590-61 (1961).

[8] Kalnins, A., "Analysis of shells of revolution subjected to symmetrical and nonsymmetrical loads," J. Appl. Mech. **31**, 467–476 (1964).

[9] Cohen, G. A., "Computer analysis of asymmetrical deformation of orthotropic shells of revolution," AIAA J. **2**, 932–934 (1964).

[10] Reissner, E., "On the theory of thin elastic shells," Reissner Anniversary Volume (J. W. Edwards, Ann Arbor, Mich., 1949) pp. 231–247.

[11] Reissner, E., "On axisymmetrical deformations of thin shells of revolution," *Proceeding of the Symposium on Applied Mathematics* (McGraw-Hill Book Company, Inc., New York, 1950), Vol. 3, pp. 27–52.

JULY 1965 AIAA JOURNAL VOL. 3, NO. 7

Uniform-Stress Spinning Filamentary Disk

A. C. KYSER*
Astro Research Corporation, Santa Barbara, Calif.

An analysis is presented for the development of the fiber patterns necessary to produce uniform fiber tension in a spinning filamentary disk. The family of fiber patterns for such isotensoid disks is described in terms of curvature, slope, and arc length, and means are suggested for obtaining polar-coordinate plots of the patterns. Included are diagrams of three of the patterns, a photograph of a model, and a discussion of the general characteristics of the family of allowable patterns. It was found that the isotensoid disk design by which the disk is covered by uniform-diameter fibers operates at half the stress of a simple hoop for a given peripheral velocity and fiber material.

Nomenclature

r = radius coordinate
r_o = radius of disk
R = r/r_o, nondimensional radius coordinate
β = angle between fiber and radius vector
ρ = radius of curvature of fiber
ω = rotation speed of disk
m' = mass per unit length along fiber
Ω = $m'\omega^2 r_o^2/T$, fiber loading parameter
F' = interfiber shear force per unit length
T = tension in structural fiber
θ = angle swept by tangent to fiber
φ = central angle coordinate
l = arc length along fiber, measured from periphery of disk
L = l/r_o, nondimensional arc length
x = R^2, nondimensional radius coordinate
s = stress in structural fiber
γ = weight density of fiber material
λ = s_{ult}/γ, specific strength of fiber
v_o = peripheral velocity of rotating disk

Introduction

THIS paper presents the analytical development of a uniform-stress (isotensoid) spinning disk composed of structural filaments of uniform cross section. The filamentary arrangement is that of a fine-mesh circular net in which the fibers form curved load-carrying paths that spiral outward from the center. It can be shown that any spiral net will carry a radially directed loading in such a way that the resultant fiber tension decreases toward the center of the net. This tension gradient is the result of the spiral load-path curvature. The fiber tension resulting from the inertia forces due to rotation, on the other hand, tends to increase toward the center. The constant-tension condition can be imposed by arranging for the curvature distribution to be that which is necessary to allow these two tension-gradient effects to cancel.

This work may be considered an extension of the work done in Refs. 1 and 2. In Ref. 1, a theory was developed for predicting equilibrium shapes of filamentary structures in which the structural loads are carried in pure tension. This paper was specifically concerned with normal loads on the fiber (i.e., pressure loads), and the solutions were presented in terms of differential equations describing the local curvature and/or slope of the structural wall in terms of the local conditions. In Ref. 2, this problem was generalized to include load components tangential to the structural wall (from centrifugal effects), and solutions for the curvature and slope equations were obtained in the form of elliptic integrals. The present paper represents a further generalization in that allowance is made for an internally generated shear stress in the filamentary wall.

This type of structure is proposed for space applications where requirements exist for large rotating surfaces in which the loads generated by the mass of rotating structure are important. One such application is suggested by Ref. 3, which discusses the use of a lightweight woven fabric net as a low-loading, low-temperature, rotating wing for re-entry deceleration. Other possible applications include the use of filamentary disks to support large surfaces for the collection or reflection of radiant energy. It is believed that an isotensoid disk of this type, in addition to having the excellent mechanical properties characteristic of filamentary structures, can be made to have a high structural efficiency.

Received June 19, 1964; revision received November 16, 1964. The work reported here was conducted with the financial support of NASA.

* Senior Engineer.

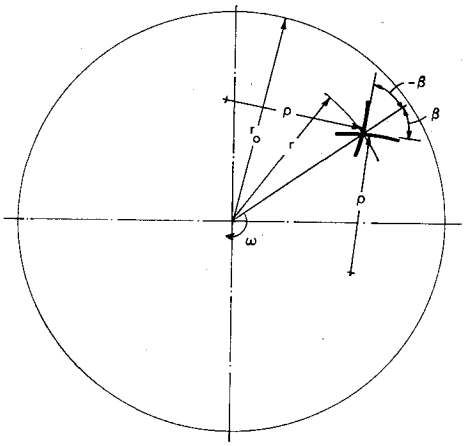

Fig. 1 Local geometry of fiber pattern.

Development of the Curvature Equation

The structure under consideration is a spinning filamentary disk having the form of symmetrical spiral net with a differentially-fine mesh, the clockwise-outward-directed fibers being attached point-by-point to the counterclockwise-outward fibers. A typical intersection between opposing fibers is shown in Fig. 1. Each branch has a local radius of curvature ρ and meets the radius vector at an angle β.

The forces acting on a differential length dl of the clockwise-outward fiber are shown in Fig. 2. The tension forces, shown dashed, are added and resolved into forces normal to and tangential to the fiber, Tdl/ρ and dT. The radially directed inertia force is $m'\omega^2 rdl$, where m' is the mass per unit length. The force $F'dl$ is the interfiber shear force, or the force exerted on the element of the clockwise-outward fiber by the corresponding counterclockwise fiber. This force must be equal and opposite to the force on the counterclockwise element at this point. For reasons of symmetry, then, it must lie in the circumferential direction normal to the radius vector.

From the diagram it can be seen that equilibrium requires that

$$m'\omega^2 rdl \sin\beta + F'dl \cos\beta = (T/\rho)dl \tag{1}$$

and

$$m'\omega^2 rdl \cos\beta - F'dl \sin\beta = (dT/dl)dl \tag{2}$$

Equations (1) and (2) can be simplified by calling

$$\Omega \equiv m'\omega^2 r_0^2/T \qquad R \equiv r/r_0 \tag{3}$$

The uniform-stress condition can be imposed by making Ω = const, assuming that the structural cross section of the fiber is proportional to the mass per unit length. If we further restrict the problem by taking m' = const (for uniform fiber size), then T = const and

$$dT/dl = 0 \tag{4}$$

Equations (1) and (2) then reduce to

$$\rho/r_0 = \sin\beta/\Omega R \tag{5}$$

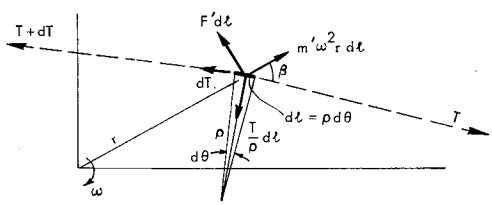

Fig. 2 Forces on fiber element.

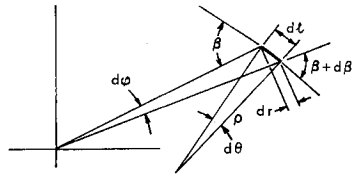

Fig. 3 Radius of curvature in polar coordinates.

and

$$F' = m'\omega^2 r/\tan\beta = (\Omega R/\tan\beta)(T/r_0) \tag{6}$$

Equation (5) is sufficient to define the geometry of the fiber pattern for any given value of the parameter Ω. It is possible to establish the family of patterns, without further analytical work, from this radius of curvature equation, by a graphical integration process using a compass and protractor.

The structural requirement for transferring shear between fibers can be seen from Eq. (6). It should be noted that the path of a given fiber need not actually follow a continuous spiral, but may follow instead a zigzag pattern, in the circumferential direction, between adjacent circles of intersections. For this type of fiber pattern, there is no tendency for the intersection to slide, and therefore there is no requirement for transferring shear.

Integration of the Curvature Equation

Equation (5) can be integrated to give a relation for ρ (or $\sin\beta$) as a function of r as follows. From Fig. 3, it can be seen that

$$d\beta = (\beta + d\beta) - \beta = d\theta - d\varphi$$

Also

$$d\theta = dr/\rho \cos\beta \qquad d\varphi = dr \tan\beta/r$$

Consequently

$$d\beta/dr = (1/\rho \cos\beta) - (\tan\beta/r)$$

or

$$(d\beta/dR) \cos\beta = (r_o/\rho) - (\sin\beta/R) \tag{7}$$

Equation (7) can, of course, be obtained from the standard form of the radius of curvature in polar coordinates. This relation can be combined directly with Eq. (5) to eliminate $d\beta/dr$ if (5) is expressed in a differentiated form:

$$\cos\beta(d\beta/dR) = (\Omega/r_o)R(d\rho/dR) + (\Omega/r_o)\rho \tag{5'}$$

Equating (5′) to (7) and substituting Eq. (5) to eliminate β gives a separable linear differential equation in $\rho(R)$:

$$2\rho d\rho/[\rho^2 - (r_0^2/2\Omega)] = -4(dR/R) \tag{8}$$

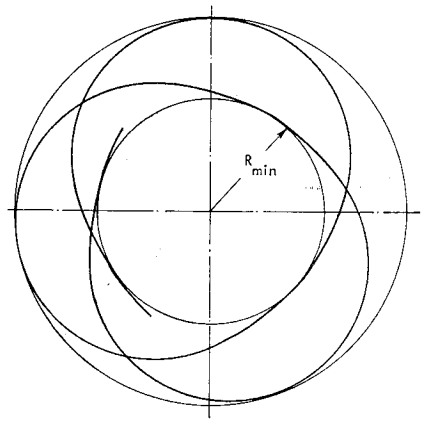

Fig. 4 Fiber pattern for isotensoid disk, $\Omega = \frac{3}{2}$.

In integrating this expression, the initial conditions are taken as those at the point at which the fiber is tangent to the outer periphery: $R = R_o = 1$, $\beta = \beta_o = \pi/2$. Here $\rho_o = r_o/\Omega$. These conditions establish the upper limits for the integration. The lower limits are taken at the generic point along the fiber curve. This process gives for the radius of curvature

$$\rho^2/r_o^2 = (1/2\Omega)\{1 + [(2 - \Omega)/\Omega](1/R^4)\} \quad (9)$$

If this expression is combined with Eq. (5), it gives

$$\sin^2\beta = (\Omega R^2/2)\{1 + [(2 - \Omega)/\Omega](1/R^4)\} \quad (10)$$

Either of Eqs. (9) or (10) suffices to describe the fiber pattern for graphical integration; Eq. (9) may be used in a step-wise forward integration with a compass, whereas Eq. (10) may be used to construct a slope field through which a continuous path may be faired.

Discussion of Curve Shape

For a complete description of the fiber pattern it would be desirable to find functions relating arc length and central angle to the radius. The arc length can be found by integrating the differential relation $dl = dr/\cos\beta$. If Eq. (10) is used to eliminate β from this relation, the result can be integrated (Ref. 4, for example) to yield the normalized arc length L:

$$L \equiv l/r_o = (1/2\Omega)^{1/2}\{(\pi/2) + \sin^{-1}[(1 - \Omega R^2)/(\Omega - 1)]\} \quad (11)$$

Given the length of fiber in the fiber pattern, it is immediately possible to compute the weight of the disk.

The central angle can be treated in similar fashion. Here the integral to be evaluated is

$$\varphi = \frac{1}{2}\int_{R^2}^{1}\left(x + \frac{C}{x}\right)[(-x^2 + Bx - C)(x^2 + C)]^{-1/2}\,dx \quad (12)$$

where $B \equiv 2/\Omega$, $C \equiv (2/\Omega) - 1$, and x is the variable of integration replacing R^2 in the integrand. Using Ref. 5, it is possible to evaluate this integral in terms of the elliptic integral of the third kind. The resulting closed-form solution for the family of fiber patterns is of questionable value here, however, because of its complexity.

Considerable insight into the nature of the fiber patterns can be obtained from examining Eqs. (9) and (10). It can be seen that there are two distinct types of curves in the one-parameter family which includes $\Omega \geq 1$. (Note that $\Omega < 1$ produces a contradiction, since it gives $\rho_o > r_o$, which requires that $r = r_o$ be a local minimum instead of maximum.) These two curve types are bounded by $\Omega = 2$; for $\Omega < 2$, ρ must increase with decreasing R, and for $\Omega > 2$, ρ must decrease. The former ($\Omega < 2$) condition produces an annular band of

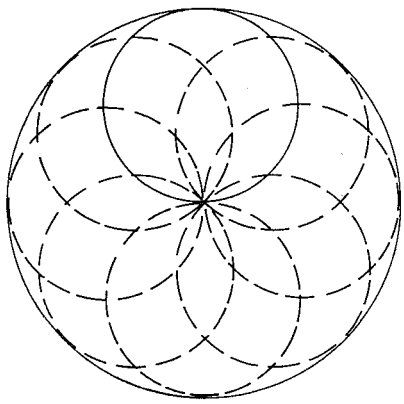

Fig. 5 Fiber pattern for isotensoid disk, $\Omega = 2$.

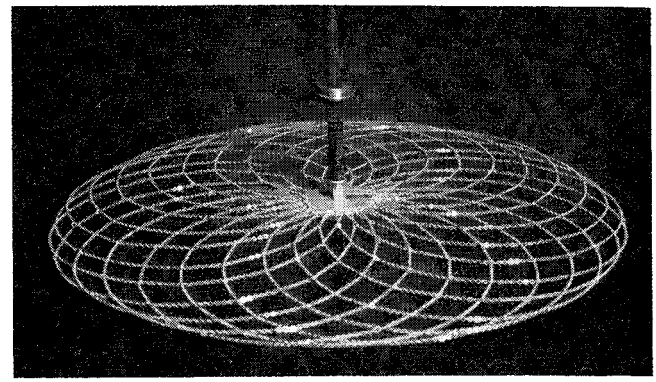

Fig. 6 Photograph of model isotensoid disk on spin stand.

fiber paths, as in Fig. 4 ($\Omega = \frac{3}{2}$), which are characterized by smooth, continuously turning curves that are tangent alternately to the outer periphery and some inner periphery. The radius of the inner periphery can be found by setting $\sin\beta = 1$ in Eq. (10). This gives

$$R_{\min}^2 = (2/\Omega) - 1 \quad (13)$$

For $\Omega = 1$, Eq. (9) gives $\rho_o = r_o$, which is simply the circular hoop.

The $\Omega = 2$ case has special importance because it is the only case that includes the origin and, therefore, covers the disk. For this case, $\rho = r_o/2 = \text{const}$, and the fiber curve is simply a circle tangent to the periphery and passing through the origin. This pattern, which is diagramed in Fig. 5, was the one chosen for the model that is photographed in Fig. 6. This pattern has the somewhat startling property that it can be mapped, without changes in arc lengths, from a rectangular net having a length-to-width ratio of 4, and consisting of square meshes at 45° to the axis of the rectangle, as shown in Fig. 7. This property arises from the fact that two circular fiber paths, whose centers are displaced on the disk by a central angle φ, intersect at values of arc length $l = 2\rho\varphi = r_o\varphi$; for a center displacement of 2φ, the arc lengths to the intersections are $l = 2r_o\varphi$; etc.

The curves $\Omega > 2$ are characterized by the fact that $\sin\beta$ and ρ both vanish at some value of R; these curves have radially-directed cusps at a value of R which can be determined by setting either ρ or $\sin\beta$ equal to zero in Eqs. (9) or (10). This gives

$$R_{\min}^4 = 1 - (2/\Omega) \quad (14)$$

Figure 8 shows the fiber pattern for $\Omega = 3$.

The $\Omega > 2$ curves are not structurally self-sufficient; each cusp must be supported by a radial force of $2T$. These radial forces could be provided by radial spokes, a hoop, or a fiber system comprised of any one of the $\Omega > 1$ curves properly

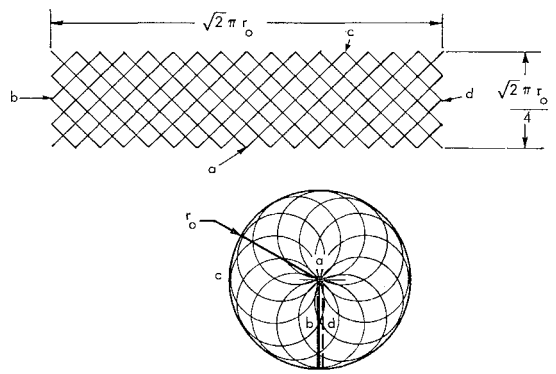

Fig. 7 Mapping of rectangular net into $\Omega = 2$ isotensoid disk.

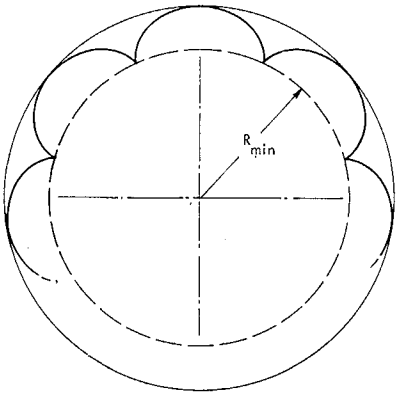

Fig. 8 Fiber pattern for isotensoid disk, $\Omega = 3$.

truncated to allow for residual radial forces at the truncation radius.

The truncation process can, of course, be applied to both the inner and outer peripheries of an annular band of a spiral net. Such a band could be spliced at its two peripheries to other similar bands (having the same fiber stress, for example). In general, these neighboring bands would each have a different reference radius r_o and a different Ω. This process, taken to the limit, could be used to produce a uniform-stress disk using tapered filaments.

The parameter Ω establishes the relation between peripheral velocity $v_o = \omega_o r_o$ and fiber stress s. The maximum peripheral velocity $(v_o)_{ult}$ of which a disk of a given material is capable can be determined by substituting the specific strength λ of the structural material for the ratio of breaking strength T_{ult} to mass per unit length as follows:

$$\lambda \equiv (s_{ult}/\gamma) \cdot (A_f/A_f) = T_{ult}/m'g \qquad (15)$$

where γ is the weight density of the material and A_f is the cross-sectional area of the fiber. If this condition is substituted into Eq. (3), which defines Ω, the ultimate velocity is seen to be

$$(v_o)_{ult} = (g\lambda\Omega)^{1/2} \qquad (16)$$

Thus a higher Ω allows a higher peripheral velocity.

If the radius of the hub is given, the choice of Ω is narrowed to a range of values given by Eq. (10) by setting $\sin^2\beta$ at the limits of 1 and 0. These values of Ω are those determined by Eqs. (13) and (14). For intermediate values of Ω, the fiber curve will intersect the hub radius at an angle β, which can be determined from Eq. (10). Since the radial component of fiber tension, $T\cos\beta$, must be carried by the hub, the load-carrying ability of the hub may be used to determine φ uniquely.

It should be recognized that the conditions governing the design of filamentary disks for use as items of hardware are likely to be such that the idealized disk analyzed here is only a point of departure. As an example, if the disk structure were required to support a reflective surface, then m' would probably be dependent on radius. For such a case, the details of the solution given here will have to be modified. The basic curvature equation is general, however, and solutions can be extracted for any set of conditions that can be defined explicitly in terms of radius.

References

[1] Schuerch, H., Burggraf, O. R., and Kyser, A. C., "A theory and applications of filamentary structures," NASA TN D-1692 (December 1962).

[2] Schuerch, H. and Burggraf, O. R., "Analytical design for optimum filamentary pressure vessels," AIAA J. **2**, 809–820 (1964).

[3] Schuerch, H. and MacNeal, R., "Low density, autorotating wings for a manned re-entry," *Engineering Problems of Manned Interplanetary Exploration* (American Institute of Aeronautics and Astronautics, New York, 1963), pp. 46–56.

[4] Pierce, B. O. and Foster, R. M., *A Short Table af Integrals* (Ginn and Co., Boston, Mass., 1957).

[5] Byrd, P. F. and Friedman, M. D., *Handbook of Elliptic Integrals for Engineers and Physicists* (Springer-Verlag, Berlin, Germany, 1954).